1,3-Hydrogen Rearrangements of Vibrationally Activated Enolate Ions in the Gas Phase

Kristin A. Sannes and John I. Brauman*

Contribution from the Department of Chemistry, Stanford University, Stanford, California 94305-5080

Received April 5, 1995[⊗]

Abstract: The unimolecular rearrangement reactions of the isomeric enolate ions of 2-butanone have been investigated using Fourier transform ion cyclotron resonance mass spectrometry and infrared multiple photon activation techniques. The individual isomers of 2-butanone enolate ions were generated from the corresponding trimethylsilyl enol ethers and photodissociated independently. Infrared multiple photon activation of the 2-butanone enolate ions induces a 1,3-hydrogen rearrangement which interconverts the individual isomers. Because infrared multiple photon activation only involves vibrational excitation, the 1,3-hydrogen rearrangement must be a thermal reaction and occur on the ground electronic state potential energy surface. The observation of a 1,3-hydrogen rearrangement is unexpected and appears to violate the Woodward−Hoffmann symmetry rules. Orbital correlation diagrams show, however, that thermal suprafacial 1,3-hydrogen rearrangements are allowed for enolic systems. Nevertheless, a more probable reaction mechanism involves the rotation of the methylene groups so that the 1,3-hydrogen rearrangement corresponds to a simple proton transfer between two unsaturated carbons.

Introduction

Mass spectrometry provides molecular weight information directly and structural information indirectly. Structural information is important because it can be used to distinguish between ions of the same nominal mass, including isomeric ions. Unimolecular rearrangement and fragmentation products are characteristic of an ion's structure. Thus, a clear understanding of the unimolecular rearrangement and fragmentation pathways can provide powerful structural information about ions, in addition to providing important insights into the reaction chemistry of ions. The unimolecular reactions of ions then can be used as a tool to predict their structures.

Deprotonation of unsymmetrical ketones can lead to a mixture of isomeric enolate ions since there are two distinct deprotonation sites (eq 1).

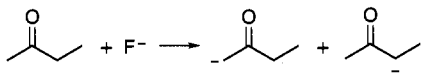

(1)

An understanding of the unimolecular fragmentations of the individual isomers can be used to distinguish between the two isomers. Because the difference in the acidities of the two deprotonation sites can be small (on the order of 2 kcal/mol), infrared multiple photon activation might be able to induce rearrangements before the enolate ions fragment. With this in mind, we began a study of the unusual unimolecular reactions of vibrationally activated enolate ions.

Bowie and co-workers have previously studied the collision-induced fragmentations of even-electron organic negative ions and proposed that intramolecular proton transfers can precede the fragmentations.[1−10] Bowie and co-workers proposed that 1,3-hydrogen rearrangements occur in the collisional activation of enolate ions (eq 2).[2]

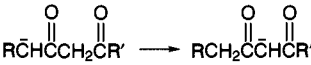

(2)

The proposed 1,3-hydrogen rearrangement is unexpected and an apparent violation of the Woodward−Hoffmann rules.[11] Thus, it is important to examine carefully the 1,3-hydrogen rearrangement in enolate ions and see if the Woodward−Hoffmann rules apply to these enolic systems. It should be determined if the rearrangement is caused by vibrational activation of the enolate ion and if the rearrangement occurs on the ground electronic state potential energy surface.

In this paper, we investigate unimolecular rearrangement reactions of the two isomeric enolate ions of 2-butanone using Fourier transform ion cyclotron resonance mass spectrometry and infrared multiple photon activation techniques. The primary and secondary enolate ions of 2-butanone were generated and photodissociated independently. Vibrational activation of 2-butanone enolate ions induces a 1,3-hydrogen rearrangement. For enolic systems, orbital correlation diagrams show that the thermal suprafacial 1,3-hydrogen rearrangements are symmetry allowed. However, a more probable pathway involves a rotation of the methylene hydrogens so that the 1,3-hydrogen rearrangement corresponds to a proton transfer between two unsaturated carbons.

[⊗] Abstract published in *Advance ACS Abstracts*, September 1, 1995.

(1) Bowie, J. H. *Mass Spectrum. Rev.* **1990**, *9*, 349−379.
(2) Bowie, J. H.; Stringer, M. B.; Hayes, R. N.; Raftery, M. J.; Currie, G. J.; Eichinger, P. C. H. *Spectrosc. Int. J.* **1985**, *4*, 277−296.
(3) O'Hair, R. A.; Bowie, J. H. *Mass Spectrom. Spec. Per. Rep., R. Soc. Chem.* **1989**, *10*, 144−180.
(4) Hayes, R. N.; Sheldon, J. C.; Bowie, J. H. *Int. J. Mass. Spectrom. Ion Processes* **1986**, *71*, 233−243.
(5) Eichinger, P. C. H.; Bowie, J. H. *Org. Mass. Spectrom.* **1987**, *22*, 103−108.
(6) O'Hair, R. A. J.; Gronert, S.; DePuy, C. H.; Bowie, J. H. *J. Am. Chem. Soc.* **1989**, *111*, 3105−3106.
(7) Stringer, M. B.; Bowie, J. H.; Eichinger, P. C. H.; Currie, G. J. *J. Chem. Soc., Perkin Trans. 2* **1987**, 385−390.
(8) Eckersley, M.; Bowie, J. H.; Hayes, R. N. *Int. J. Mass. Spectrom. Ion Processes* **1989**, *93*, 199−213.
(9) Raftery, M. J.; Bowie, J. H. *Int. J. Mass. Spectrom. Ion Processes* **1988**, *85*, 167−186.
(10) Adams, G. W.; Bowie, J. H.; Hayes, R. N. *J. Chem. Soc., Perkin Trans. 2* **1989**, 2159−2167.
(11) Woodward, R. B.; Hoffmann, R. *The Conservation of Orbital Symmetry*; Academic Press, Inc.: New York, 1971.

0002-7863/95/1517-10088$09.00/0

Experimental Section

Chemicals. Nitrogen trifluoride was purchased from Ozark Mahoning and 2-butanone was purchased from Aldrich. Both chemicals were used without further purification. All neutrals were degassed on the forelines by several freeze−pump−thaw cycles before introduction into the high-vacuum chamber.

Synthesis of Trimethylsilyl Enol Ethers. The primary and secondary trimethylsilyl enol ethers of 2-butanone were synthesized by modifying the procedure outlined by House et al.[12] For the primary trimethylsilyl enol ether of 2-butanone, diisopropylamine (55 mmol) and *n*-butyllithium (50 mmol) were added to 50 mL of dry distilled THF at 0 °C maintained under nitrogen. This solution was cooled to −78 °C using a dry ice/acetone bath and 2-butanone (50 mmol) was added slowly. After 5 min, trimethylsilyl chloride (55 mmol) was syringed in. The solution was allowed to warm slowly to room temperature. The solution then was washed four times with cold aqueous sodium bicarbonate and once with a cold saturated sodium chloride solution. The solution was dried and distilled. The primary trimethylsilyl enol ether of 2-butanone was isolated by preparative gas chromatography (Hewlett-Packard 5790 gas chromatograph equipped with a thermal conductivity detector, 10% SE-30 on Chrom WHP 80/100 mesh column at 90 °C). The structure of the primary trimethylsilyl enol ether of 2-butanone was confirmed by the observation of the vinyl hydrogens, the methyl hydrogens, and the methylene hydrogens in the 200-MHz NMR spectrum. No peaks corresponding to the secondary isomer were observed in the NMR spectrum.

For the secondary trimethylsilyl enol ether of 2-butanone, 2-butanone (125 mmol) was added to a solution of trimethylsilyl chloride (150 mmol) and triethylamine (300 mmol) in 50 mL of dimethylformamide. This mixture was refluxed for 48 h. The mixture was then cooled and diluted with 100 mL of pentane. The resulting solution was washed in rapid succession with cold aqueous 1.5 M HCl and cold acqueous sodium bicarbonate. The pentane layer was dried, concentrated, and distilled. The secondary trimethylsilyl enol ether of 2-butanone was isolated by preparative gas chromatography under the same conditions as the primary trimethylsilyl enol ether of 2-butanone. The secondary trimethylsilyl enol ether of 2-butanone is a mixture of the *E* and *Z* isomers (eq 3). The 200-MHz NMR spectrum shows two types of vinyl hydrogens and four types of methyl hydrogens, consistent with a roughly equal mixture of the *E* and *Z* isomers. No peaks corresponding to the primary isomer were observed in the NMR spectrum.

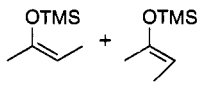

(3)

Ion Generation. The primary ion, F^-, was generated from electron impact on nitrogen trifluoride (eq 4). Reaction of the primary trimethylsilyl enol ether of 2-butanone with F^- generated the primary enolate ion of 2-butanone (eq 5); no secondary enolate ion is formed.[13] Reaction of the secondary trimethylsilyl enol ether of 2-butanone with F^- generated the secondary enolate ion of 2-butanone (eq 6, only one isomer is shown for convenience); no primary enolate ion is formed.[13] These reactions were complete in 200−300 ms. An impurity peak due to trimethylsiloxide anion was observed and ejected prior to infrared multiple photon activation. Based on the bond dissociation energies

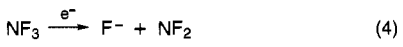

(4)

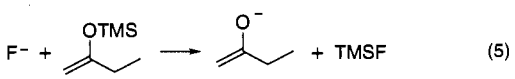

(5)

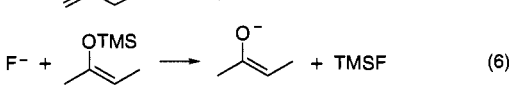

(6)

of Si−O bonds (90 kcal/mol) and Si−F bonds (154 kcal/mol) and the electron affinities of F^- (78 kcal/mol), the primary 2-butanone enolate ion (41 kcal/mol) and the secondary 2-butanone enolate ion (39 kcal/mol), the exothermicity of eq 5 is approximately 27 kcal/mol and the exothermicity of eq 6 is approximately 25 kcal/mol.[13,14]

Instrumentation. All experiments were performed with a Fourier transform ion cyclotron resonance mass spectrometer (FT-ICR)[15] equipped with impulse excitation and controlled by the IonSpec OMEGA system.[16−18] The analyzer cell was modified so that it was possible to do photochemical experiments. In order to allow the laser beam to enter the cell, the front excitation plate was replaced with a plate that has a $^7/_8$ in. mesh-covered hole. The back excitation plate was replaced with a molybdenum mirror to reflect the laser beam back out. Typical operating conditions were the following: −1.20 trapping voltage, 3.0 amp filament current, 3 eV electron energy, and 0.8 T magnetic field. Pressures of the neutrals in the analyzer cell were monitored with a nude ion gauge (Granville-Phillips 307). The background pressure was $\sim 2 \times 10^{-8}$ Torr. Typical operating pressures were $1.2-2.0 \times 10^{-7}$ Torr for NF_3 and $2-3 \times 10^{-7}$ Torr for the trimethylsilyl enol ethers of 2-butanone. The total operating pressure was $3.2-5 \times 10^{-7}$ Torr.

A tunable pulsed CO_2 laser (Lumonics 103−2 CO_2 TEA laser) was used for the infrared multiple photon activation experiments. Only the 9.6 μm, R(22) branch, corresponding to a wavelength of 1079.85 (3.1 kcal/mol per photon), was used. The laser wavelength was measured by a CO_2 laser spectrum analyzer (Optical Engineering Model 16-A). The laser beam spot size is reduced by an iris before entering the analyzer cell through a potassium chloride window that is transparent at the laser wavelength. The intensity of the laser beam can be attenuated by passing the beam through CaF_2 flats of varying thicknesses. Because the laser beam is reflected back through the ion cloud by a molybdenum mirror, the effective fluence is twice the measured fluence. The energy of the laser pulse was measured using a Scientech 365 power and energy meter with a Scientech 38−0102 volume-absorbing disk calorimeter. The area of the laser beam spot is calculated from the image left by the laser pulse on thermal paper. The fluence (J/cm^2) is calculated by dividing the laser pulse energy (in J) by the area (in cm^2) of the laser beam spot and then multiplying by two. The range of measured laser fluences was 4−6.5 J/cm^2.

Reproducibility. The quantitative results are based on a small number of working days (1−2) in which quantitative data with a high degree of reproducibility were obtained. Several different data sets of multiple scans were obtained at each different fluence value. The reproducibility of these photoproduct yields was within ±1−2%. Additional attempts at data acquisition were made for each compound and qualitative agreement (photoproduct yields within 10−15% of reported values) was observed. The low degree of reproducibility was due to instability in the ion signal prior to irradiation and/or misalignment of the laser beam. Because of possible systematic errors and experimental difficulties associated with the interaction of the high-intensity laser pulse with the analyzer cell, an estimate of the absolute accuracy of the photodissociation yield measurements is taken to be within approximately ±5%. However, some cancellation of errors should occur for the photoproduct branching ratios. It is important that the basic conclusions of this paper are not strongly dependent on the quantitative results. The basic conclusions are drawn from the absence or presence of a specific photoproduct and the relative abundances of the photoproducts.

Calculations. Two types of semiempirical calculations were performed. The π-system was studied using Hückel molecular orbital calculations. All atoms in the π-system were treated identically; distinguishing between carbon, oxygen, and hydrogen atoms by modifying the coulomb and bond integrals does not change the outcome of the calculation. A general orbital correlation diagram was constructed for the suprafacial 1,3-hydrogen rearrangement of enolic systems.

(12) House, H. O.; Czuba, L. J.; Gall, M.; Olmstead, H. D. *J. Org. Chem.* **1969**, *34*, 2324.

(13) The work of Squires and DePuy shows that the trimethylsilyl enol ether method generates specific isomers (Squires, R. R.; DePuy, C. H. *Org. Mass. Spectrom.* **1982**, *17*, 187).

(14) Zimmerman, A. H.; Reed, K. J.; Brauman, J. I. *J. Am. Chem. Soc.* **1977**, *99*, 7203.

(15) Marshall, A. G.; Verdun, F. R. *Fourier Transforms in NMR, Optical, and Mass Spectrometry: A User's Handbook*; Elsevier: New York, 1990.

(16) McIver, R. T., Jr.; Hunter, R. L.; Baykut, G. *Rev. Sci. Instrum.* **1989**, *60*, 400.

(17) McIver, R. T., Jr.; Hunter, R. L.; Baykut, G. *Anal. Chem.* **1989**, *61*, 489.

(18) McIver, R. T., Jr.; Baykut, G.; Hunter, R. L. *Int. J. Mass. Spectrom. Ion Processes* **1989**, *89*, 343.

Table 1. Photoproduct Yields for the Primary and Secondary Enolate Ions of 2-Butanone

enolate ion	fluence (J/cm²)	neutral product lost			
		H_2	CH_4	C_2H_6	C_2H_4
$C^-H_2C(=O)CH_2CH_3$	6.5	34.4	7.5	47.5	10.6
	4.3	68.5	6.5	15.3	9.7
$CH_3C(=O)C^-HCH_3$	6.5	52.4	2.7	39.4	5.5
	4.3	77.5	2.8	15.2	4.5

The AM1 calculations were done with MOPAC version 6.00.[19,20] The transition state geometry for the suprafacial 1,3-hydrogen rearrangement was calculated by forcing the geometry to correspond to a hydrogen moving in the plane perpendicular to the plane of the carbons, oxygen, and methylene hydrogens. Another transition state geometry was calculated using a combination of the saddle point subroutine and the TS algorithm. For each geometry, a "force-calculation" was performed to determine how many negative vibrational frequencies existed.

Results

In the infrared multiple photon activation of the primary and secondary enolate ions of 2-butanone, the same four fragmentation products and vibrational-induced electron detachment were observed. In each case, there is ~45% electron detachment and ~3% fragmentation. The decrease in the total ion intensity that occurs in the spectra taken with the laser on is attributed to electron detachment. It was not possible to achieve mass balance between the "laser off" spectra and the "laser on" spectra. The four fragmentation channels are as follows: (1) ethane loss to produce deprotonated ketene anion; (2) ethylene loss to produce acetaldehyde enolate ion; (3) methane loss to produce deprotonated methylketene anion; and (4) hydrogen loss to produce 3-buten-2-one enolate ion.[21] The neutral products are inferred based on mass balance and thermochemical considerations.

For both the primary and secondary enolate ions of 2-butanone, the ratio of products observed was found to be highly fluence dependent (see Table 1). For the primary enolate ion of 2-butanone, the loss of ethane (~48%) was competitive with the loss of hydrogen (~34%) at the highest fluence (6.5 J/cm²) while hydrogen loss (~69%) dominated at the lowest fluence (4.3 J/cm²). Similarly, for the secondary enolate ion of 2-butanone, the loss of ethane (~39%) was competitive with the loss of hydrogen (~52%) at the highest fluence (6.5 J/cm²), while hydrogen loss (~78%) dominated at the lowest fluence (4.3 J/cm²).

Discussion

1,3-Hydrogen Rearrangement in 2-Butanone Enolate Ion. In our experiments, we know *a priori* which isomer of the 2-butanone enolate ion is initially generated and that the isomer is stable under the conditions of its generation.[13,22] Infrared multiple photon activation of the primary and the secondary 2-butanone enolate ions gives the same four fragmentation products plus vibrationally-induced electron detachment. The two fragmentation products corresponding to ethane and ethylene loss come from the primary 2-butanone enolate ion while the two fragmentation products corresponding to hydrogen and methane loss come from the secondary 2-butanone enolate ion.[21] Fragmentation products from both isomers are observed even though only a single isomer is generated originally. Thus, infrared multiple photon activation induces a 1,3-hydrogen rearrangement which converts the primary 2-butanone enolate ion into the secondary 2-butanone enolate ion and vice versa. Because each isomer gives a different ratio of fragmentation products, an equilibrium between the two isomers is not reached in both cases. We believe that the rearrangement channel and the fragmentation channels are competitive and that the rate constants for the fragmentation channels are larger than the rate constant for the rearrangement channel.

Lowest Energy Channel. We can learn about the ordering of the channels by studying the fluence dependence of the ratio of the fragmentation products. In infrared mutliple photon activation, an ion absorbs photons until a unimolecular reaction rate constant is competitive with the absorption rate constant. If the ion is just below the point at which a reaction is possible, absorption of an additional photon can cause the reaction to occur. Because the absorption of one photon increases the energy of an ion by ~3 kcal/mol, the ions will fragment over an energy range of at least 3 kcal/mol. Unimolecular reaction rate constants increase with increasing internal energy. On the other hand, the absorption rate constant is relatively insensitive to the internal energy of the ion; it is proportional to the laser intensity and the ion's absorption cross section. In our laser experiments, the laser fluence is roughly proportional to the laser intensity.[23] Thus, the absorption rate constant is proportional to the laser fluence. By changing the laser fluence and thus the absorption rate constant, the reaction channels that have reaction rate constants that are competitive with the absorption rate constant can be selected. At a low laser fluence and thus at a slow absorption rate constant, reaction channels with low activation energies and small *A*-factors will be competitive with the absorption rate constant and can dominate. On the other hand, at a high laser fluence and thus at a fast absorption rate constant, reaction channels with high activation energies and large *A*-factors are competitive with the absorption rate constant and will dominate.

The infrared multiple photon dissociation of the primary and secondary enolate ions of 2-butanone are fluence dependent. For the primary 2-butanone enolate ions, more rearrangement occurs at the lowest fluence (75%) than at the highest fluence (41%). On the other hand, for the secondary 2-butanone enolate ions, less rearrangement appears to occur at the lowest fluence (20%) than at the highest fluence (45%). In addition, when the primary enolate ions are collisionally activated using multiple low energy collisions, the only observable channel is vibrationally-induced electron detachment.[24,25] Since no fragmentation products are observed, it cannot be determined if rearrangement is taking place.

The above observations are consistent with the schematic representation of the potential energy surface in Figure 1; the vibrationally-induced electron detachment channel is not shown. Either rearrangement or vibrationally-induced electron detachment is probably the lowest energy channel; both occur before the fragmentation channels. Although the rate constants for all channels are competitive, the rate constant for rearrangement increases more slowly with increasing internal energy than do the rate constants for the fragmentation channels. This is

(19) Coolidge, M. B.; Stewart, J. J. P. MOPAC, Ver. 6.0. *QCPE*; 445: 1990.

(20) Dewar, M. J. S.; Zoebisch, E. G.; Healy, E. F.; Stewart, J. J. P. *J. Am. Chem. Soc.* **1985**, *107*, 3902.

(21) Sannes, K. A.; Brauman, J. I. Manuscript in preparation.

(22) Nibbering and Noest showed that thermalized enolate ions are stable with respect to 1,3-hydrogen rearrangements (Noest, A. J.; Nibbering, N. M. M. *Int. J. Mass Spectrom. Ion Phys.* **1980**, *34*, 383–385).

(23) In our laser experiments, the laser pulse has two components: a high intensity spike that lasts 150–200 ns and a 3-ms tail which can be approximated as a rectangular pulse. Since most of the products are formed during the tail of the laser pulse, we treat the laser pulse as if it had constant intensity. Therefore, we can argue that the laser fluence is proportional to the laser intensity.

(24) Boering, K. E.; Brauman, J. I. *Int. J. Mass. Spectrom. Ion Processes* **1992**, *117*, 357–386.

(25) Boering, K. E.; Rolfe, J.; Brauman, J. I. *Rapid Commun. Mass Spectrom.* **1992**, *6*, 303–305.

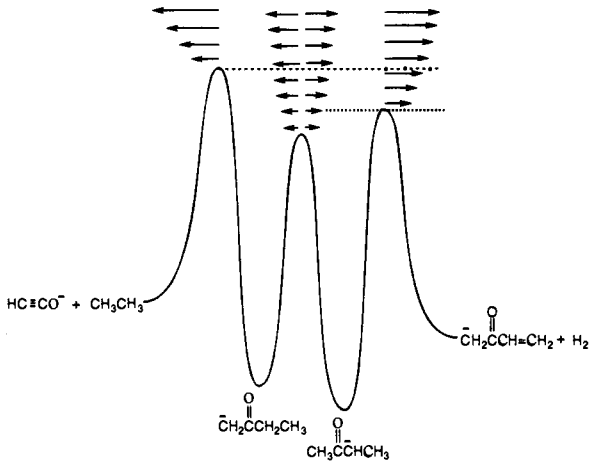

Figure 1. Schematic representation of the potential energy surface for the 1,3-hydrogen rearrangement and fragmentation channels of the primary and secondary enolate ions of 2-butanone. For a general description of the infrared multiple photon activation of the primary and secondary 2-butanone enolate ions see refs 31 and 32. This figure is not drawn to scale.

consistent with what is known about the behavior of other rearrangement reactions (i.e. low activation energies and small *A*-factors). The activation energy for the fragmentation of the secondary enolate ion of 2-butanone is smaller than the activation energy for the fragmentation of the primary enolate ion of 2-butanone. The difference in activation energies cannot be too large, otherwise fragmentation products for both enolate ions would not be observed at all fluences. The absorption rate constants for the two isomers must be similar since the total amount of fragmentation is similar for each isomer.

In the low fluence case of the infrared multiple photon activation of the primary 2-butanone enolate ion, the energy range of the excited ions goes just above the primary 2-butanone enolate ion fragmentation threshold (dashed line in Figure 1). Most of the primary 2-butanone enolate ions would rearrange to secondary 2-butanone enolate ions and fragmentation products from the secondary 2-butanone enolate ion would be expected to dominate. In the high fluence case, all of the ions are probably pumped above the primary 2-butanone enolate ion fragmentation threshold. Fragmentation and rearrangement of the primary 2-butanone enolate ions would be competitive, but the fragmentation products of the primary 2-butanone enolate ion would be expected to dominate over the fragmentation products of the secondary 2-butanone enolate ions.

In the low fluence case of the infrared multiple photon activation of the secondary 2-butanone enolate ion, the energy range of the excited ions goes just above the primary 2-butanone enolate ion fragmentation threshold. Fragmentation products from the secondary 2-butanone enolate ion would be expected to dominate. In other words, although rearrangement is occurring, most of the primary 2-butanone enolate ions are not formed with enough energy to fragment. Thus, the majority of rearrangements are not detected and less rearrangement appears to occur in the low fluence case. In the high fluence case, all of the ions are probably pumped above the primary 2-butanone enolate ion fragmentation threshold. Fragmentation and rearrangement of the secondary 2-butanone enolate ions would be competitive, but the fragmentation products of the secondary 2-butanone enolate ion would be expected to dominate over the fragmentation products of the primary 2-butanone enolate ions.

It is difficult to estimate thermochemically the heats of formation for the transition states. The heat of formation of the transition state for the fragmentation of the primary 2-butanone enolate ion can be estimated by calculating the enthalpy change for the reaction of primary 2-butanone enolate ion going to ketene radical anion and ethyl radical. The heat of formation for ketene radical anion is not known but the electron affinity of ketene is small, so the enthalpy change for the reaction of primary 2-butanone enolate ion going to ketene and ethyl radical was used as an upper bound; complexation energy was not taken into account.[26] This gives a heat of formation of ~70 kcal/mol. The heat of formation of the transition state for the fragmentation of the secondary 2-butanone enolate ion is estimated by calculating the enthalpy change for the reaction of a secondary enolate ion going to 3-buten-2-one and a hydride ion; complexation energy is not taken into account. This gives a heat of formation of ~57 kcal/mol. The estimated 13 kcal/mol difference in the stabilities of the two transition states is too large to fit the experimental observations. However, it does indicate that the transition state for fragmentation from the secondary 2-butanone enolate ion is probably more stable than the transition state for fragmentation from the primary 2-butanone enolate ion which is consistent with experimental observations.

Reaction Pathway. Absorption of infrared photons causes vibrational excitation, so the infrared multiple photon induced 1,3-hydrogen rearrangement is occurring on the ground electronic state potential energy surface. The energy of the ion is increased in approximately 3-kcal/mol increments (the energy of one infrared photon). Thus, the rearrangement can occur before the threshold for a fragmentation channel has been reached, and the observed fragmentation reactions will occur close to the fragmentation threshold. On the other hand, the collisional activation experiments of Bowie and co-workers were carried out under high-energy single-collision conditions. Consequently, most of the decomposing ions are excited well above the reaction thresholds for all the channels.

Orbital Correlation Diagrams. The 1,3-hydrogen rearrangement is one of the prototype sigmatropic processes analyzed by Woodward and Hoffmann.[11] Geometrical constraints require the hydrogen to be transferred on the same side of the π-system (suprafacial). The reaction involves an avoided state crossing and has a substantial barrier; it is described as symmetry forbidden.

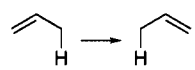

Surprisingly, the apparently similar enolic rearrangement does not have an avoided crossing and is, by the usual definition, symmetry allowed, see Figure 2.

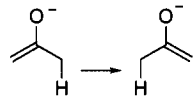

Calculations at the AM1 level, however, suggest that although the simple concerted sigmatropic reaction is allowed by symmetry, it proceeds through a rather different process. The suprafacial transition state geometry does not correspond to a stationary point on the 1,3-hydrogen rearrangement potential energy surface of the acetone enolate ion. A "force-calculation" showed that the geometry has two negative frequencies and thus corresponds to an inflection point on the potential energy surface. Consequently, a transition state geometry for the 1,3-hydrogen rearrangement potential energy surface was calculated using a combination of the saddle point and TS subroutines of MOPAC. The optimized geometry of the transition state has

(26) The electron affinity for the ethyl anion is negative which makes it unclear as to what the heat of formation of the ethyl anion actually means.

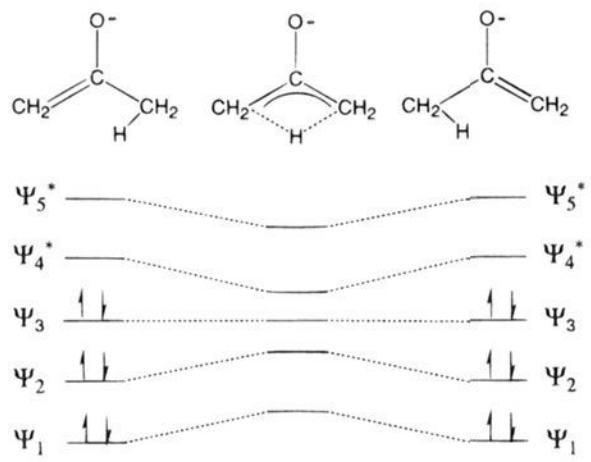

Figure 2. Orbital correlation diagram for the suprafacial 1,3 hydrogen rearrangement in the enolic system of acetone enolate ion constructed from Hückel calculations. The migrating atom is actually above the plane of the paper.

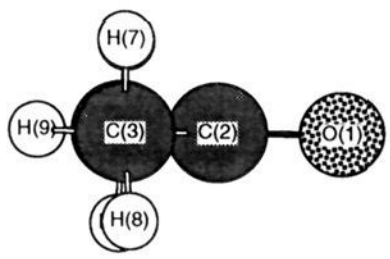

Figure 3. Side view of the transition state for 1,3-hydrogen rearrangement in the enolic system of acetone enolate ion from AM1 calculations. The migrating hydrogen (H(9)) is in the plane of the carbons and oxygen and the methylene hydrogens (H(5), H(6), H(7), H(8)) are 90° to the plane of the carbons and oxygen.

the migrating hydrogen almost in the plane of the carbons and the oxygen and the methylene hydrogens are perpendicular to the plane of the carbons and the oxygen (Figure 3). This transition state geometry has the charge localized on the methylene group and the 1,3-hydrogen rearrangement corresponds to a simple proton transfer between two unsaturated carbons. This AM1 calculated transition state geometry is similar to the *ab initio* calculations by Bowie.[4] A "force-calculation" showed that this transition state had only one negative frequency and corresponds to a transition state on the 1,3-hydrogen rearrangement potential energy surface. An internal reaction coordinate calculation also showed that the transition state relaxes back to the acetone enolate ion geometry. Thus, rotation of the methylene groups followed by proton transfer is an allowed rearrangement pathway. Consistent with the experimental observation that the rearrangement channel is competitive with the fragmentation channel, AM1 calculates that the barrier for this rearrangement (~59 kcal/mol) is below the barrier to fragmentation (~72 kcal/mol). The barrier to this rearrangement is due to the rotation of the methylene group as well as the migration of the hydrogen.

Competitive Reaction Pathways. In order for the mechanism for the rearrangement discussed above to be plausible, it must be possible for the methylene groups to rotate. This requires that some of the vibrational energy of the enolate ion be distributed into the torsional mode of the methylene group. The vibrational excitation of the methylene torsional mode has been proposed in the mechanism for vibrationally-induced electron detachment which is experimentally observed in addition to the 1,3-hydrogen rearrangement.[27,28] The 1,3-hydrogen rearrangement process must be competitive with the vibrationally-induced electron detachment since both are observed.

Vibrationally-induced electron detachment occurs when the potential energy surface for the acetone enolate ion and the potential energy surface for the acetone enolate radical are close enough that vibrational−electronic coupling occurs. The energy surface of acetone enolate ion is highly dependent on the angle between the methylene hydrogens and the plane containing the carbons and oxygen. When the methylene hydrogens are in the same plane as the carbons and the oxygen, the charge is delocalized and the threshold for electron detachment corresponds to the electron affinity of the acetone enolate radical (41 kcal/mol).[14] When the methylene hydrogens are perpendicular to the plane of the carbons and oxygen, however, the charge is localized on the methylene group and is only stabilized through the inductive effects of the carbonyl group. The threshold for electron detachment can be approximated by the electron affinity of the methyl radical (1.8 kcal/mol).[29] When the methylene hydrogens are perpendicular to the plane of the carbons and oxygen, the acetone enolate ion and acetone radical potential energy surfaces will be close together so that coupling of the acetone enolate ion to the radical plus electron continuum could be efficient. The rate constant for methylene rotation was estimated by RRKM theory to 10^9 s^{-1}. On the other hand, the upper limit for the electron detachment rate constant was estimated[27,28] to be 10^7 s^{-1}. Thus, even though rotation of the methylene group is relatively efficient, the electron detachment process is very inefficient. Consequently, a proton transfer reaction could be competitive with vibrationally-induced electron detachment.

The barrier to rotation of the methylene group is approximately 39 kcal/mol (the difference in the stability of the delocalized acetone enolate ion and the localized acetone enolate ion). Since the barrier to forming the methyl anion−ketene complex is[27,28] approximately 60 kcal/mol and the barrier to the 1,3-hydrogen rearrangement must be lower than the barrier to formation of the complex, the barrier to proton transfer can be at most 20 kcal/mol. Proton transfer reactions can be moderately efficient even when there is a barrier to the reaction.[30]

Conclusions

Upon infrared multiple photon activation, 2-butanone enolate ions undergo a 1,3-hydrogen rearrangement. The thermal suprafacial 1,3-hydrogen rearrangement is symmetry allowed in enolic systems. However, a more plausible reaction mechanism involves the rotation of the methylene group perpendicular to the plane of the carbons and the oxygen so that the 1,3-hydrogen rearrangement corresponds to a simple proton transfer between two unsaturated carbons.

Acknowledgment. We are grateful to the National Science Foundation for support of this work.

JA951103Y

(27) Foster, R. F.; Tumas, W.; Brauman, J. I. *J. Phys. Chem.* **1989**, *93*, 61.

(28) Foster, R. F.; Tumas, W.; Brauman, J. I. *J. Chem. Phys.* **1983**, *79*, 4644−4646.

(29) Ellison, G. B.; Engelking, P. C.; Lineberger, W. C. *J. Am. Chem. Soc.* **1978**, *100*, 2556−2558.

(30) Han, C. C.; Brauman, J. I. *J. Am. Chem. Soc.* **1989**, *111*, 6491.

(31) If the primary 2-butanone enolate ion is pumped to just below its fragmentation threshold (dashed line in Figure 1), the primary 2-butanone enolate ion would rearrange to the secondary 2-butanone enolate ion and only fragmentation products from the secondary 2-butanone enolate ion would be observed. Once the primary enolate ion is pumped above its fragmentation threshold (dashed line in Figure 1), fragmentation products from both the primary and secondary enolate ions of 2-butanone would be observed. The relative amounts of the different fragmentation products would depend on how far above the fragmentation threshold the ions are pumped.

(32) If the secondary 2-butanone enolate ion is pumped to just above its fragmentation threshold (dotted line in Figure 1), only the fragmentation products from the secondary 2-butanone enolate ions would be observed. Similarly, if the secondary 2-butanone enolate ion is pumped to just below the fragmentation threshold for the primary 2-butanone enolate ion (dashed line in Figure 1), only the fragmentation products from the secondary 2-butanone enolate ion would be observed. However, this does not mean that rearrangement is not occurring in each case. Rearrangement to the primary 2-butanone enolate ion would not be detected because fragmentation of the primary 2-butanone enolate ion can only occur at higher energies. When the secondary 2-butanone enolate ion is pumped above the fragmentation threshold for the primary 2-butanone enolate ion (dashed line in Figure 1), fragmentation products from both enolate ions would be observed.